

Effect of 3d Impurities on the Superconducting Transition Temperature of the Layered Compound NbSe₂

J. J. Hauser, M. Robbins, and F. J. DiSalvo

Bell Laboratories, Murray Hill, New Jersey 07974

(Received 14 February 1973)

The transition temperature of NbSe₂ as a function of the concentration of such paramagnetic impurities as Fe, Ni, and Co shows a very strong anomaly close to the critical concentration which destroys superconductivity. The strength of the effect in NbSe₂ is believed to be caused both by the weak depairing of the impurities and by their nonstatistical distribution resulting from the layered structure.

An anomalous dependence of the superconducting transition temperature on paramagnetic impurities has been observed in La_{1-x}Gd_x¹ and in La_{3-x}Gd_xIn² and was explained in terms of magnetic ordering by Bennemann.³ In the case of La_{1-x}Gd_x,¹ the effect was somewhat obscured by the fact that two crystalline modifications (hcp and fcc) usually coexist in La. On the other hand, the basis for magnetic ordering was well established in these alloys by the fact that while superconductivity disappears at a concentration of about 1-at. % Gd, the alloys become ferromagnetic⁴ above 1 °K at a concentration of 2.5-at. % Gd. In the case of La_{3-x}Gd_xIn,² the compound La₃In is cubic but there is no study showing long-range magnetic order in the more concentrated alloys.

A recent structural study⁵ of $M_x\text{NbSe}_2$ ($x = \frac{1}{4} - \frac{1}{2}$), where M is one of the transition metals (Ti, V, Cr, Mn, Fe, Co, Ni), showed that all these metals but Ti enter the octahedral holes between the prismatic Se layers. The maximum concentration as established from the change in lattice parameter is between $x = \frac{1}{3}$ and $x = \frac{1}{2}$. The magnetic properties⁶ of these intercalated compounds showed that all the transition-metal atoms which enter the lattice except Co had a localized magnetic moment and one of the compounds (Fe_{0.28}NbSe₂) showed antiferromagnetic ordering at 120 °K. Consequently, these alloys are ideally suited for a study with a dilute concentration of impurities.

All the samples of $M_x\text{NbSe}_2$ (where M is Fe, Ni, Co, Zn, or Al) were prepared separately from the elements by reacting at 800 °C for 48 h pressed pellets of the appropriate mixtures in sealed evacuated quartz tubes.⁵ At the conclusion of the heating cycle the quartz tubes were examined visually and showed no sign of free selenium on the sides of the tube. This indicates that the reaction in the tube was complete yielding materials in good agreement with the desired stoichiometry. All of the materials were examined using a Norelco x-ray diffractometer with CuK α radiation. All samples were found to be single phase with the desired 2H-

NbSe₂ structure. Unit-cell parameters which obey Vegard's law (Table I) were found to be consistent with the previously reported lattice-parameter study.⁵ Certain compositions were obtained in the single-crystal form using vapor transport in a closed tube with iodine as the carrier. The transition temperatures of the samples were obtained by susceptibility measurements using a sensitive ac bridge with two balanced coils. The bridge was operated at 10 000 Hz with 4 V which corresponds to a modulating field of 6 G.

On the basis of the layered structure of this compound, one expects a nonrandom nonstatistical (in the sense that the different atomic environments in the Se and Nb layers preclude the random statistical distribution of a normal substitutional or interstitial alloy) distribution of impurities.⁷ This simply results from the fact that when a certain number of impurities are intercalated in a certain layer, the lattice parameter is locally affected⁵ and consequently, subsequent impurities will be located in the same layer rather than in a new one. This will lead, as we shall see, to the broadening and scatter of any property measured as a function of impurity concentration. The determination of the transition temperature is further complicated by the fact that even in the pure compounds, it is strongly affected by nonstoichiometry⁸: A 0.88-at. % deficiency in Se decreases the transition temperature of 2H-NbSe₂ from 7 to 6.1 °K. The transition temperature (T_{c0}) of the present 2H-NbSe₂ samples as defined by the onset of the superconducting signal was 7 °K; as shown in Fig. 1, the transition extends over 0.65 °K down to 6.35 °K, at which point the sample was fully superconducting. The transition temperatures of the alloys (T_c) were even broader most probably as a result of combining the nonstoichiometry with the nonstatistical distribution of the impurities. The transition widths in Al and Zn alloys ranged from 0.5 to 1 °K; the same was usually true for the Fe, Ni, and Co alloys except in the vicinity of the anomaly where transitions as wide as 2 °K were observed. Typical transition

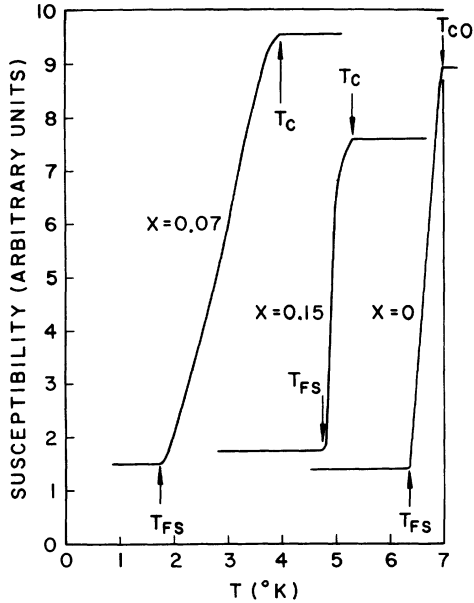


FIG. 1. Typical transition curves (susceptibility vs temperature) for various Co_xNbSe_2 alloys; the transition for pure NbSe_2 is shown as $x=0$. T_c is defined as the onset of superconductivity, T_{FS} is the temperature where the sample is fully superconducting and the width of transition is $\Delta T = T_c - T_{FS}$.

curves are shown in Fig. 1 for a dilute Co alloy ($x=0.015$) and for a Co alloy in the anomalous concentration range ($x=0.07$). The same curves were observed for Ni and Fe alloys in the dilute and

anomalous concentration regions. The transition temperatures reported in the figures of the present study are defined by the onset of superconductivity (T_c in Fig. 1); as it is impossible to separate the effect of nonstoichiometry from the nonstatistical distribution of impurities, this criterion was chosen in order to compare the T_c of alloys with the literature value⁸ of 7 °K for the T_{c0} of NbSe_2 . As we shall show later, regardless of the scatter and the width of the transitions, the anomaly is large enough that its presence does not depend on the criterion chosen for T_c .

The transition temperatures for the alloys investigated are shown as a function of impurity concentration in Fig. 2. First of all, it is clear that in the case of Al which is an s - p band metal and of Zn which has a full d band and where therefore, no local moment is expected in both cases, T_c can be seen to be a monotonically decreasing function of impurity concentration. In the dilute range ($x \leq 0.07$) the decrease is linear in both cases and the slope dT_c/dc (where c is the impurity concentration in at.%) is equal to 1.3 °K/at.% which is typical for a nonlocalized nonmagnetic impurity. Above $x=0.07$, T_c falls more rapidly in the case of Al; although this effect is not clearly understood it may be caused by a nonstatistical distribution becoming more severe close to the concentration where superconductivity vanishes or perhaps by the greater valency of Al. Furthermore, while transition-metal atoms occupy octahedral holes,⁵ it was shown⁹ that Al and Cu atoms occupy tetrahedral holes (the same most probably applies to Zn).

TABLE I. Unit-cell parameters of materials in the system $M_x\text{NbSe}_2$ where $M = \text{Fe}, \text{Ni}, \text{Co}, \text{Zn}, \text{Al}$.

$M_x\text{NbSe}_2$		a	c	$M_x\text{NbSe}_2$		a	c
$M = \text{Fe}$	$x = 0.005$	3.44(4)	12.55(2)	$M = \text{Al}$	$x = 0.04$	3.44(7)	12.55(8)
	0.0075	3.44(4)	12.55(4)		0.06	3.44(9)	12.56(3)
	0.01	3.44(4)	12.55(6)		0.08	3.45(1)	12.56(7)
	0.0125	3.44(5)	12.55(6)		0.10	3.45(2)	12.57(3)
$M = \text{Ni}$	$x = 0.01$	3.44(4)	12.54(8)	$M = \text{Zn}$	$x = 0.01$	3.44(4)	12.55(6)
	0.02	3.44(5)	12.54(2)		0.05	3.44(6)	12.58(8)
	0.03	3.44(5)	12.53(8)		0.07	3.44(7)	12.59(3)
	0.04	3.44(5)	12.53(2)		0.09	3.44(7)	12.60(1)
	0.05	3.44(5)	12.52(5)				
	0.06	3.44(6)	12.52(0)				
	0.07	3.44(7)	12.51(2)				
$M = \text{Co}$	$x = 0.01$	3.44(4)	12.54(7)				
	0.03	3.44(5)	12.53(1)				
	0.04	3.44(5)	12.52(2)				
	0.05	3.44(5)	12.51(7)				
	0.06	3.44(6)	12.51(0)				
	0.07	3.44(6)	12.50(3)				
	0.08	3.44(6)	12.49(8)				
	0.09	3.44(6)	12.49(0)				

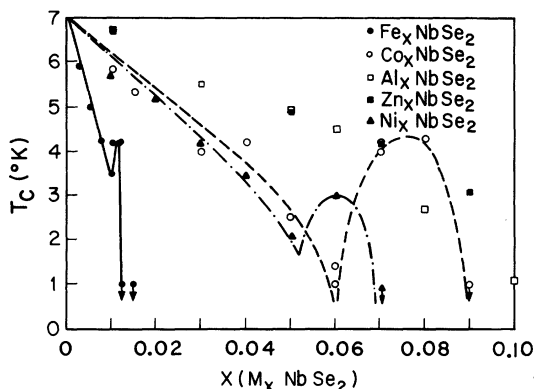


FIG. 2. Dependence of the transition temperature T_c on the number x of impurity moles M where $M = \text{Fe, Ni, Co, Al, or Zn}$. The data points at 1°K with the downward arrows indicate samples still normal at 1°K which is the lowest temperature of measurement.

This difference should not in principle greatly affect T_c .

The data for Fe, Ni, and Co alloys shown in Fig. 2 reveal a striking anomaly: Close to the concentration where T_c vanishes, T_c can be seen to increase with impurity concentration, pass through a maximum, and decrease again. In the case of Co, the anomaly is quite striking in the sense that T_c is below 1°K (lowest attainable temperature) at $x = 0.06$ before dropping again below 1°K at $x = 0.09$. The dilute portion of the data can again be approximated by a straight line with a slope of dT_c/dc of $3^\circ\text{K/at.}\%$ for Co and Ni and $11^\circ\text{K/at.}\%$ for Fe. These values compare quite well with rare-earth local-moment systems with T_c anomalies: dT_c/dc was $3^\circ\text{K/at.}\%$ for Gd in La_3In^2 and $5^\circ\text{K/at.}\%$ for Gd in La.⁴ On the other hand, the effect of Fe in the chalcogenide is much weaker than in other systems: For Fe, $dT_c/dc \approx 50\text{--}200^\circ\text{K/at.}\%$ in transition-metal alloys and compounds.^{10,11} The weaker depairing effect of Fe in NbSe_2 may result from the fact that the Nb layers which are primarily responsible for superconductivity are somewhat shielded from the impurities by the Se layers. This weaker depairing is what enables us to observe the anomaly.

The anomaly which occurs at $x = 0.01$ for Fe_xNbSe_2 is firmly established in two ways. First, the dilute portion of the curve ($x < 0.01$) shows little scatter; second, the two very close data points shown at $x = 0.01125$ in Fig. 2 are the result of two separate experiments starting from freshly weighted powders. The reproducibility in the peak region is therefore convincing evidence for the validity of the anomaly. The greater width of the superconducting transition in the vicinity of the anomaly mentioned above is quite understandable from the narrow concentration width of this anomaly.

Indeed, the peak only extends from $x = 0.01$ to $x = 0.0125$ and even ignoring stoichiometry and distribution problems, it is very difficult because of the small amounts of impurity involved to guarantee the concentration to such an accuracy. As a matter of fact, the accuracy in concentration is about $x = \pm 0.005$ thus explaining why at $x = 0.01$, T_c can be either 3.5 or 4.2°K . Single crystals of Fe_xNbSe_2 were measured resistively but as it was not possible to assert the Fe concentration because of the transport reaction, the data are not included in Fig. 2. The resistive measurements agreed with the susceptibility measurements to the extent that a nominal $\text{Fe}_{0.0125}\text{NbSe}_2$ crystal did not display a resistive superconducting transition above 1°K .

The data for the Co alloys show appreciably more scatter than the data obtained on Fe alloys. The magnitude of the anomaly is, however, so large that the scatter is rather unimportant. It is interesting to notice that after superconductivity almost vanishes at $x = 0.06$, it goes through a maximum with a T_c value approximately equal to that obtained with nonmagnetic impurities (Al, Zn). One also notices in Fig. 2 that while the concentration width of the anomaly is very narrow for Fe_xNbSe_2 , it is quite wide for Co_xNbSe_2 . As discussed by Ben-nemann,³ such an anomaly occurs when the impurity spins are no longer free to rotate as a result of ordering; this results in a reduction of spin-flip scattering and thus in an increase in T_c . The rapid decrease of T_c following the anomalous slow decrease and increase of T_c arises from an interplay of spin-orbit scattering and gliding of the Fermi surface. One could therefore explain the different width of the anomalies in Fe and Co alloys by assuming that spin-orbit scattering is stronger in Co_xNbSe_2 than in Fe_xNbSe_2 , thus preventing Fermi-surface gliding until much higher concentrations; this would permit the reduction in spin-flip scattering (which tends to increase T_c) to take its full effect in the Co alloys. One could, on the other hand, assume that the intrinsic anomaly should be quite sharp for both Fe and Co alloys and that the broadening is introduced by the weak depairing of Fe and Co (which is weaker for Co) and by the non-statistical distribution of impurities (which again is worse for Co as shown by the greater scatter in the dilute range). The nonstatistical distribution of impurities would mean that certain impurity atoms are already ordered while others still allow spin-flip scattering.

The data for the Ni alloys fall between those for Fe and Co alloys, but closer to the data for the Co alloys. This is consistent with the fact that both Co and Ni are expected to have a lower spin value than Fe⁶ (the situation for Co will be discussed in greater detail later on).

The data for Fe, Ni, and Co are shown in a nor-

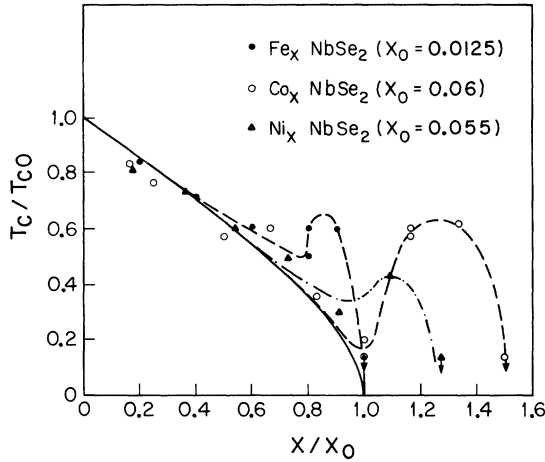


FIG. 3. Dependence of the reduced transition temperature T_c/T_{c0} (where T_{c0} is the transition temperature of pure NbSe_2) on reduced number of impurity moles (where x_0 is the critical number of impurity moles defined in the text). The solid line represents the Abrikosov-Gor'kov theory (Ref. 12).

malized plot in Fig. 3. The dependence of the reduced transition temperature is plotted versus reduced concentration and the dashed curves are simply drawn through the experimental points. The critical number of impurity moles ($x_0 = 0.0125$ for Fe, $x_0 = 0.055$ for Ni, and $x_0 = 0.06$ for Co) and the solid curve are determined from¹²

$$\ln T_c/T_{c0} = \psi\left(\frac{1}{2}\right) - \psi\left[\frac{1}{2} + 0.140 T_{c0}(x/T_c x_0)\right] \quad (1)$$

by fitting the experimental results at low impurity concentrations, where the impurity spins are free to rotate. In relation (1), ψ is the digamma function, T_c and T_{c0} are, respectively, the transition temperatures of the alloys $M_x\text{NbSe}_2$ and pure NbSe_2 , and x is the number of impurity moles. Although the Abrikosov-Gor'kov (AG) theory [Eq. (1)] was derived for a random distribution of noninteracting spins, we are applying it here to a system where the impurity distribution was described above as nonrandom. It is felt, however, that the distribution is only nonrandom on an atomic scale (i.e., on the scale of the layers) but can be considered as approximately random on a microscopic or semi-macroscopic scale (i.e., when one considers several layers together). The fact that the data for Fe, Ni, and Co can be reduced in the dilute range to fit approximately the AG curve (Fig. 3) is a justification of the previous assumption. The critical concentrations ($c_0 = 0.41$ -at.% Fe, $c_0 = 1.8$ -at.% Ni, and $c_0 = 2$ -at.% Co) are of the same order as those found in $\text{La}_{1-x}\text{Gd}_x$ (0.82 at.%)¹ and in $\text{La}_{3-x}\text{Gd}_x\text{In}$ (2.15 at.%)² In terms of Bennemann's theory,³ it is clear from Fig. 3 that spin-orbit scattering is important in Fe, Ni, and Co alloys

as the first effect of ordering is a reduction in spin-flip scattering which results in a deviation towards higher reduced transition temperatures from the Abrikosov-Gor'kov curve¹² (solid line in Fig. 3).

Since the existence of a Co moment is implied in this work by the existence of the anomaly in T_c and since earlier work suggested no moment,⁶ we measured the susceptibility of several Co_xNbSe_2 compounds. $2H\text{-NbSe}_2$ shows a large Pauli paramagnetic susceptibility¹³ that is temperature dependent above 100 °K, but is temperature independent below 100 °K, except for a small impurity Curie "tail" that is apparent at temperatures below ≈ 30 °K. In order to obtain the Co moment in Co_xNbSe_2 we used only the data below 100 °K, since a temperature dependence in the susceptibility above 100 °K could be ascribed not only to Co moments but also to the large Pauli paramagnetism of these compounds. Between 4.2 and 100 °K, the susceptibility of the Co_xNbSe_2 compounds was well described by $\chi = C/(T + \theta) + \chi_p$, where from C we obtain the local moment on the Co (μ_{eff}) in the usual way,¹⁴ and χ_p represents the temperature-independent part of the susceptibility. For the dilute alloys of Co ($0 < x < 0.1$) we found for $x = 0.03$, $\mu_{\text{eff}} = 0.40\mu_B$, $\theta = 2$ °K; for $x = 0.05$, $\mu_{\text{eff}} = 0.33\mu_B$, $\theta = 0$ °K; for $x = 0.09$, $\mu_{\text{eff}} = 0.50\mu_B$, $\theta = 4$ °K. Non-zero θ values can arise either from a Kondo interaction of the Co moments with conduction electrons or from Co-Co interactions (or both), and thus interpreting the above measured θ values as a function of x is difficult. Any interpretation of these results is further complicated by the fact that the density of states in the conduction band of NbSe_2 is very high and has a peak close to the Fermi level,¹⁵ and it is not clear how the band structure or the Fermi level is affected by the addition of Co.

In the aforementioned previous study,⁶ the susceptibility of $\text{Co}_{0.27}\text{NbSe}_2$ was found to be temperature independent between 500 and 60 °K; a small increase in the magnetization below 60 °K was attributed to impurities. It turns out, however, that the temperature-independent susceptibility was the result of small clumps and clusters of ferromagnetic Co¹⁶ and of the large Pauli susceptibility. If, however, one subtracts the temperature-independent part of the susceptibility, the susceptibility below 60 °K is approximately proportional to T^{-1} and yields $\mu_{\text{eff}} = 0.8\mu_B$ and a θ value close to 0 °K. This result is in good agreement with the susceptibility measurements on the dilute alloys used in the present study. These results show that the local moment increases slightly with increasing Co concentration, but increases discontinuously at the superlattice concentration ($\mu_{\text{eff}} = 3.66\mu_B$ at $x = 0.33$).¹⁷ The small value of μ_{eff} for $x < 0.1$ is consistent with the fact that the dT_c/dc value for

Co is only twice as large as that of nonmagnetic elements (Al, Zn). In the Fe and Ni compounds, the local moments are close to the expected free-ion (spin-only) values. Ni has a much larger moment than Co,⁶ but the effect upon T_c is about the same for both indicating that the conduction-electron-impurity spin coupling is much weaker in Ni than in Co. Finally, Co with a localized magnetic moment also removes the required valence state of quenched Co^{3+} which corresponds to an unlikely oxidation state for the Co ion in chalcogenides. We may now

speculate on the valence state of Co: Unquenched Co^{3+} ($S=2$) can be ruled out as this would imply that Co is as magnetic as Fe^6 ; unquenched Co^{2+} ($S=\frac{3}{2}$) is rather unlikely in view of the very small spin value reported above. Finally, quenched Co^{3+} ($S=0$) can be ruled out as Co has a localized moment, which leaves us with the most probable valence state of quenched Co^{2+} ($S=\frac{1}{2}$).

The authors would like to thank V. G. Lambrecht, Jr., J. V. Waszcek, and J. Bernardini for their technical assistance.

¹R. A. Hein, R. L. Falge, Jr., B. T. Matthias, and E. Corenzwit, *Phys. Rev. Lett.* **2**, 500 (1959).

²J. E. Crow and R. D. Parks, *Phys. Lett.* **21**, 378 (1966).

³K. H. Bennemann, *Phys. Rev. Lett.* **17**, 438 (1966).

⁴B. T. Matthias, H. Suhl, and E. Corenzwit, *Phys. Rev. Lett.* **1**, 92 (1958).

⁵J. M. Voorhoeve-van den Berg and R. C. Sherwood, *J. Solid State Chem.* **1**, 134 (1970).

⁶J. M. Voorhoeve-van den Berg and R. C. Sherwood, *J. Polym. Sci.* **32**, 167 (1970).

⁷J. A. Wilson (private communication), using electron microscopy, observed that Co was not uniformly distributed among the layers.

⁸E. A. Antonova, S. A. Medvedev, and I. Yu. Shebalin, *Zh. Eksp. Teor. Fiz.* **57**, 329 (1969) [*Sov. Phys.-JETP* **30**, 181 (1970)].

⁹J. M. Voorhoeve, *J. Less-Common Met.* **26**, 399 (1972).

¹⁰A. M. Clogston, B. T. Matthias, M. Peter, H. J. Williams, E. Corenzwit, and R. C. Sherwood, *Phys. Rev.* **125**, 541 (1962).

¹¹T. H. Geballe, B. T. Matthias, B. Caroli, E. Corenzwit, J. P. Maita, and G. W. Hull, *Phys. Rev.* **169**, 457 (1968).

¹²A. A. Abrikosov and L. P. Gor'kov, *Zh. Eksp. Teor. Fiz.* **39**, 1781 (1960) [*Sov. Phys.-JETP* **12**, 1243 (1961)].

¹³M. Marezio, P. D. Dernier, A. Menth, and G. W. Hull, Jr., *J. Solid State Chem.* **4**, 425 (1972).

¹⁴J. S. Smart, *Effective Field Theories of Magnetism* (Saunders, Philadelphia, Pa., 1966).

¹⁵M. H. van Maaren and H. B. Harland, *Phys. Lett. A* **29**, 571 (1969); and band calculations by L. F. Mattheiss (unpublished).

¹⁶R. C. Sherwood (private communication).

¹⁷K. G. Verhoeven, Ph.D. thesis (Leiden University, 1971) (unpublished).

Effect of Hydrostatic Pressure on Superconducting Lead-Indium Alloys Using Electron Tunneling

H. H. Hansen,*† R. L. Pompi, and T. M. Wu

Department of Physics, State University of New York at Binghamton, Binghamton, New York 13901

(Received 27 December 1972)

The effect of pressure on the effective phonon spectrum $\alpha^2(\omega)F(\omega)$, the dimensionless electron-phonon interaction strength λ , and the average electron-phonon coupling function $\langle \alpha^2 \rangle$ has been determined in the superconducting alloys $\text{Pb}_{95}\text{In}_5$ and $\text{Pb}_{88}\text{In}_{12}$. Electron-tunneling measurements at pressures from 0 to 3600 bar provided the energy gap and tunneling density of states which served as input to McMillan's gap inversion program which calculated $\alpha^2(\omega)F(\omega)$, λ , and $\langle \alpha^2 \rangle$. Pressure production was via solid helium which provided nearly hydrostatic pressures. The energy gap decreases and the phonon frequencies increase with increasing pressure. The impurity band undergoes the smallest relative shift with increasing pressure and the transverse peak exhibits the largest relative shift. $\alpha^2(\omega)F(\omega)$ shifts toward higher frequencies and decreases slightly in amplitude. The net result of all these effects is for a shift of the electron-phonon interaction toward weaker coupling. The best indicators of this trend are the observed decrease of λ and $\langle \alpha^2 \rangle$ with increasing pressure. These values are $d\lambda/dP = -7.9 \times 10^{-6} \text{ bar}^{-1}$ and $d\langle \alpha^2 \rangle/dP = -3.2 \times 10^{-6} \text{ bar}^{-1}$ for $\text{Pb}_{88}\text{In}_{12}$. The values for $\text{Pb}_{95}\text{In}_5$ are close to these. The pressure dependence of γ , the electronic-specific-heat coefficient, determined from the pressure dependence of the quantity $Z_n(0) = 1 + \lambda$, gives a value close to that of Pb determined from thermal-expansion measurements and from recent theoretical considerations.

I. INTRODUCTION

The effect of pressure on superconductivity for bulk properties such as the transition temperature

T_c and the critical magnetic field H_c is well established.¹⁻⁴ The effect of pressure on such microscopic properties as the strength of the electron-phonon interaction and phonon spectrum is much